

# Spectral Gamma-ray Signatures of Cosmological Dark Matter Annihilations

Lars Bergström, Joakim Edsjö

*Department of Physics, Stockholm University, SCFAB, SE-106 91 Stockholm, Sweden*

Piero Ullio

*SISSA, via Beirut 4, 34014 Trieste, Italy*

We propose a new signature for weakly interacting massive particle (WIMP) dark matter, a spectral feature in the diffuse extragalactic gamma-ray radiation. This feature, a sudden drop of the gamma-ray intensity at an energy corresponding to the WIMP mass, comes from the asymmetric distortion of the line due to WIMP annihilation into two gamma-rays caused by the cosmological redshift. Unlike other proposed searches for a line signal, this method is not very sensitive to the exact dark matter density distribution in halos and subhalos.

PACS numbers: 95.35.+d; 14.80.Ly; 98.70.Rz

It has been known since long that particle dark matter annihilations may produce an observable gamma-ray line [1–6]. One of the prime particle dark matter candidates is a WIMP (Weakly Interacting Massive Particle), of which the supersymmetric neutralino is a favourite example. WIMP annihilation into  $\gamma\gamma$  and  $Z\gamma$  would give monochromatic gamma rays with an energy equal to (or close to) the WIMP mass [3,5,6]. Since these gamma rays are monochromatic and have high energy they would constitute a spectacular signature of annihilating dark matter.

There has been a rapid development of the understanding of how structure forms in the Universe. In the current model for structure formation, the  $\Lambda$ CDM model, most of the matter is in the form of non-relativistic cold dark matter (CDM), but with a contribution to the energy density also from a cosmological constant ( $\Lambda$ ). As shown by detailed  $N$ -body simulations (see, e.g., [7,8] and references therein), in such a picture large structures form by the successive merging of small substructures, with smaller objects generally being denser. The  $N$ -body simulations also show that the dark matter density profile in clusters of galaxies and in single galaxies develops a steep cusp near the center,  $\rho_{CDM}(r) \sim r^{-\alpha}$  with  $\alpha$  ranging from 1 [9] to 1.5 [10].

At present, it is not clear whether these  $N$ -body predictions are in agreement or not with available data. On large scales, this scenario gives excellent agreement with observations, see, e.g., the prediction of the Lyman- $\alpha$  absorption lines at high redshifts [11]. On smaller scales, one of the main puzzles is how to properly include baryonic matter. For instance, it appears that the contradiction between the number of satellites found in the  $N$ -body simulation of a halo with the size of the Milky Way and the number of those observed may be explained by plausible mechanisms which make most small subhalos dark [12]. It is less clear how to get agreement between the measured rotation curves of dwarf and low surface brightness galaxies and those found in  $\Lambda$ CDM simulations (see [13] for a recent review).

Here we will take the view that the  $\Lambda$ CDM picture is basically correct and that structure forms hierarchically, with the number density of halos of mass  $M$  being distributed as  $dN/dM \propto M^{-\beta}$  with  $\beta \sim 1.9 - 2$ , as predicted by Press-Schechter theory [14] and also verified in  $N$ -body simulations. Furthermore, we will use that the concentration of halos grows with decreasing mass.

Previous analyses (e.g., [15–20]) have focused on the dark matter gamma-ray signals from the Galactic center and the halo of the Milky Way or isolated nearby galaxies and satellites; in these cases the actual dark matter distribution within halos plays a crucial role for the observability. The presence of substructures, as well as of central cusps, increases the detected rates [15,17–19], but still it may be difficult to resolve such individual sources (see [18]). We now show that the integrated signal of unresolved cosmological dark matter halos gives a potential detection method which is more robust to changes of the details of how the dark matter is distributed locally.

We consider the lightest neutralino,  $\chi$ , of the MSSM (the Minimal Supersymmetric Standard Model) as our template particle. The mass range is from around 50 GeV up to several TeV (see [21] for a recent review). We start with the (unrealistic) case of all the dark matter being smoothly distributed at all redshifts, and then modify the results by introducing structure. The comoving number density  $n_c$  of neutralinos, after decoupling from chemical equilibrium (“freeze-out”) at very large temperatures ( $T \sim m_\chi/20$ ) is depleted slightly due to self-annihilations, governed by the Boltzmann equation  $\dot{n}_c = -\langle\sigma v\rangle(1+z)^3 n_c^2$ , where  $\langle\sigma v\rangle$  is the thermally-averaged annihilation rate, which, to an excellent approximation after freeze-out, is velocity independent, since the neutralinos move non-relativistically.

Each of the  $\chi$  particles that disappears will give rise to  $N_\gamma$  photons on the average, with an energy distribution in the rest frame of the annihilation

$$\frac{dN_\gamma(E)}{dE} = \frac{dN_{\text{cont}}}{dE}(E) + b_{\gamma\gamma}\delta(m_\chi - E), \quad (1)$$

where the first term gives the average continuum gamma

ray distribution per annihilating  $\chi$  and the second term is the  $\gamma\gamma$  line contribution, with  $b_{\gamma\gamma}$  being the branching ratio into  $\gamma\gamma$  (in this discussion, we neglect the  $Z\gamma$  channel [6]).

Gamma-rays observed today with an energy  $E_0$  correspond to an emitted energy  $E = (1+z)E_0$ . If we now track, using the Boltzman equation, the number of neutralinos that have disappeared from redshift  $z$  until now, and fold in the energy distribution Eq. (1), we can estimate the diffuse extragalactic gamma ray flux. Let  $H_0$  be the Hubble parameter. Using the relation between time and redshift (see, e.g., [22])  $d/dt = -H_0(1+z)h(z)d/dz$  with  $h(z) = \sqrt{\Omega_M(1+z)^3 + \Omega_K(1+z)^2 + \Omega_\Lambda}$ , where  $\Omega_M$ ,  $\Omega_\Lambda$  and  $\Omega_K = 1 - \Omega_M - \Omega_\Lambda$  are the present fractions of the critical density given by matter, vacuum energy and curvature, the rate is

$$\frac{dn_c(z)}{dz} = \kappa \frac{(1+z)^2}{h(z)} n_c(z)^2, \quad (2)$$

where  $\kappa = \langle\sigma v\rangle/H_0$ .

The differential spectrum of the number density  $n_\gamma$  of photons generated by annihilations is given by:

$$\frac{dn_\gamma}{dz} = N_\gamma \frac{dn_c}{dz} = \int_0^{m_\chi} \frac{dN_\gamma(E)}{dE} \frac{dn_c}{dz} dE. \quad (3)$$

Here,  $dn_c/dz$  can be computed directly from (2) to excellent accuracy, replacing the exact solution  $n_c(z)$  by the present number density of neutralinos  $n_0$  on the right hand side.

Approximating  $\Omega_\chi \sim \Omega_M$ , we obtain  $n_0 = \rho_\chi/m_\chi = \rho_{\text{crit}}\Omega_M/m_\chi$ , where  $\rho_{\text{crit}} = 1.06 \cdot 10^{-5} h^2 \text{ GeV}/\text{cm}^3$  and  $h$  is the Hubble parameter in units of  $100 \text{ km s}^{-1} \text{ Mpc}^{-1}$ , and we find that the gamma-ray flux is given by:

$$\phi_\gamma = \frac{c}{4\pi} \frac{dn_\gamma}{dE_0} = 8.3 \cdot 10^{-14} \text{ cm}^{-2} \text{ s}^{-1} \text{ sr}^{-1} \text{ GeV}^{-1} \times \frac{\Gamma_{26} \Omega_M^2 h^3}{m_{100}^2} \int_0^{z_{up}} dz \frac{(1+z)^3 e^{-z/z_{\text{max}}} dN_\gamma(E_0(1+z))}{h(z) dE}. \quad (4)$$

where we defined  $\Gamma_{26} = \langle\sigma v\rangle/(10^{-26} \text{ cm}^3 \text{ s}^{-1})$  and  $m_{100}$  the mass in units of 100 GeV. The term  $e^{-z/z_{\text{max}}}$  accounts for absorption of gamma-rays along the line of sight. For the energies we are interested in,  $1 \text{ GeV} \lesssim E_0 \lesssim 500 \text{ GeV}$ , it is the starlight and (poorly known) infrared background radiation which is the limiting factor. An optical depth of order unity is reached for a redshift which can be approximated by  $z_{\text{max}}(E_0) \sim 3.3(E_0/10 \text{ GeV})^{-0.8}$ , which is a simplified representation of the results of [23,24]. The exponential form is a good approximation for small values of  $z_{\text{max}}$  as in most of our cases. The upper limit of integration is  $z_{up} = m_\chi/E_0 - 1$ , since the maximum rest frame energy of a photon in an annihilation event is  $E = m_\chi$ . The gamma line contribution to (4) is particularly simple, just picking out the integrand at  $z+1 = m_\chi/E_0$ ; it has the very distinctive and

potentially observable signature of being asymmetrically smeared to lower energies (due to the redshift) and of suddenly dropping just above  $m_\chi$ . The continuum emission will produce a less conspicuous feature, a smooth ‘‘bump’’ below one tenth of the neutralino mass which may be more difficult to detect. To give an example of the results, we performed a large scan of the MSSM parameter space obtained with the DarkSUSY package [25]. Models with large  $\gamma\gamma$  rates ( $(\sigma v)_{2\gamma} \gtrsim 10^{-29} \text{ cm}^3 \text{ s}^{-1}$ ) exist in all the mass range from  $m_\chi = 70 \text{ GeV}$  to several TeV. Consider a high-rate model with  $m_\chi = 86 \text{ GeV}$ ,  $\Gamma_{26} \sim 6$ ,  $b_{\gamma\gamma} \sim 3 \cdot 10^{-3}$ , in the ‘‘concordance’’ cosmology  $\Omega_M = 0.3$ ,  $\Omega_\Lambda = 0.7$ ,  $h = 0.65$  (see Ref. [19] for the full range of predicted fluxes in the MSSM). The continuous gamma-ray rest frame energy distribution per annihilating particle comes mainly from hadronization and decay of  $\pi^0$ s and is conveniently parametrized as  $dN_{\text{cont}}(E)/dE = (0.42/m_\chi) e^{-8x}/(x^{1.5} + 0.00014)$  where  $x = E/m_\chi$ . The resulting flux near 86 GeV is around  $10^{-15} \text{ cm}^{-2} \text{ s}^{-1} \text{ sr}^{-1} \text{ GeV}^{-1}$ , some five orders of magnitude below the diffuse extragalactic flux extrapolated from the Energetic Gamma-Ray Experiment Telescope (EGRET) measurements [26].

We now include the important effects of structure formation. Consider a halo of mass  $M$  whose radial density profile can be generically described by [20]  $\rho_{DM}(r) = \rho'_{DM} f(r/a)$ , with  $\rho'_{DM}$  being a characteristic density and  $a$  a length scale. These are found in  $N$ -body simulations not to be independent parameters, as smaller halos are associated with higher densities. We assume that the halo of mass  $M$  accreted from a spherical volume of radius  $R_M$ , determined by requiring that the average cosmological density times that volume is equal to  $M$ ,  $\rho_0 \cdot 4\pi R_M^3/3 = M$  (with  $\rho_0 \sim 1.3 \cdot 10^{-6} \text{ GeV}/\text{cm}^3$ ). The increase of average squared overdensity per halo (which is what enters the annihilation rate) is given by:

$$\Delta^2 \equiv \left\langle \left( \frac{\rho_{DM}}{\rho_0} \right)^2 \right\rangle_{r < R_M} = \left( \frac{\rho'_{DM}}{\rho_0} \right) \frac{I_2}{I_1}, \quad (5)$$

where  $I_n \equiv \int_0^{R_M/a} y^{2n} dy (f(y))^n$ . Here the dependence on the upper limit of integration is rather weak, while for the lower limit of  $I_2$ , in very singular profiles, like the Moore profile, a cut-off has to be imposed due to rapid self-annihilations near the center [20].

Computing  $I_2/I_1$  numerically, and using values of  $\rho'_{DM}/\rho_0$  as determined for Milky Way size halos from [20], we find values of  $\Delta^2$  of  $2.3 \cdot 10^5$  for the Moore profile,  $1.5 \cdot 10^4$  for the Navarro-Frenk-White (NFW) profile [9], and  $7 \cdot 10^3$  for a cored, modified isothermal profile (modified such that the density falls as  $1/r^3$  at large radii [20]). The flux ratios, 30 : 2 : 1 for these three models should be compared with the ratios 1000 : 100 : 1 obtained within a 5-degree cone encompassing the galactic center [20].

We also take into account that the number density of halos is scaling like  $\sim 1/M^2$ , and that small-mass halos

are denser. Again, we resort to the highest-resolution  $N$ -body simulations available to date. Fitting the concentration parameter of Moore-type halos by [20]  $c \sim 100 (M_{\text{vir}}/h^{-1}M_{\odot})^{-0.084}$ , we find to a good approximation  $\Delta^2 \sim 2 \cdot 10^5 M_{12}^{-0.22}$ , where  $M_{12}$  is the halo mass in units of  $10^{12}$  solar masses. This means that the total flux from a halo of mass  $M$  scales as  $M^{0.78}$ . Since the number density of halos goes as  $M^{-2}$ , the fraction of flux coming from halos of mass  $M$  scales as  $M^{-1.22}$ . Thus the gamma-ray flux will dominantly come from the smallest CDM halos. In simulations, substructure has been found on all scales (being limited only by numerical resolution). For very small dark matter clumps, however, no gain in overdensity is expected, since once the matter power spectrum enters the  $k^{-4}$  region a constant density is predicted [18]. We conservatively set  $10^5 - 10^6 M_{\odot}$  as the minimal scale.

Finally, regarding redshift dependences, we have assumed a constant enhancement factor  $\Delta^2$  out to  $z \sim 1$ , and have arbitrarily imposed quadratic growth in the enhancement factor from  $z \sim 10$  to the fully developed epoch  $z = 1$ . (The observable feature is not sensitive to this assumption.) Furthermore, in Eq. (4) we make the replacement  $(1+z)^3 \rightarrow 1$  [27], reflecting the fact that we are now dealing with a clumped, rather than a smooth distribution with density scaling  $\sim (1+z)^3$ .

We thus arrive at the following expression for the flux including structure formation

$$\phi_{\gamma} = \frac{c}{4\pi} \frac{dn_{\gamma}}{dE_0} = 8.3 \cdot 10^{-14} \text{ cm}^{-2} \text{ s}^{-1} \text{ sr}^{-1} \text{ GeV}^{-1} \times \frac{\Gamma_{26} \Omega_M^2 h^3}{m_{100}^2} \int_0^{z_{\text{up}}} dz \frac{\Delta^2(z) e^{-z/z_{\text{max}}}}{h(z)} \frac{dN_{\gamma}(E_0(1+z))}{dE}. \quad (6)$$

We find that the flux from small Moore-like halo structure is enhanced by roughly a factor  $2 \cdot 10^6$  compared to the smooth case, giving observability for the same annihilation parameters as used above. In Fig. 1, we show the results for the same 86 GeV MSSM model as in the example above, and a model of 166 GeV mass,  $\Gamma_{26} = 59$ ,  $b_{\gamma\gamma} = 1.2 \cdot 10^{-4}$ .

Several remarks are in order here.

(a) The flux calculated here is made up by the integrated effect of a large number of halos. One could also detect nearby clumps in the Galactic halo [20,19]. This would in particular make the line even more visible.

(b) Contrary to previous expectations (e.g., [28]), we do not find it excluded that a large part of the measured extragalactic gamma-ray flux around and above 10 GeV may originate from WIMP annihilations. Our more optimistic conclusion rely primarily on three factors: (1) The improved understanding of CDM structure formation, through semianalytic and numerical methods showing that less massive halos are denser. (2) The possibility that the density profile of each subhalo can be steep, increasing further the emissivity. (3) The observability is

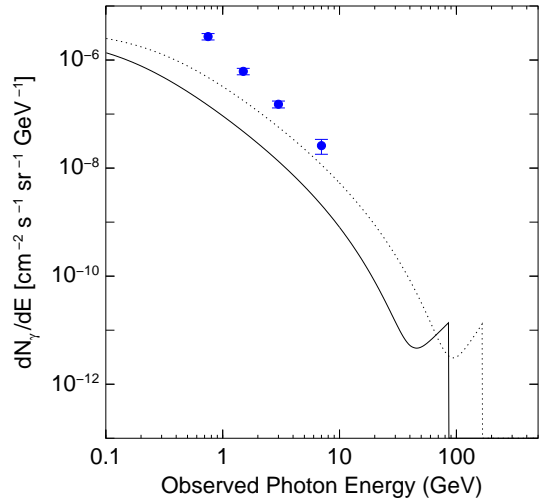


FIG. 1. The predicted diffuse  $\gamma$ -ray flux, from cosmic annihilations into continuum gamma-rays, and a gamma-ray line. The redshifted line gives the conspicuous feature at the highest energies. Shown are cosmic annihilation of 86 GeV (solid line) and 166 GeV (dotted line) neutralinos. A Moore density profile for the halo substructure has been assumed. The EGRET data [26] on the extragalactic flux are the data points with error bars shown.

helped by the existence of a sharp gamma-ray line in the annihilation spectrum and the expected opacity of the universe to this signal at the energies considered here, which gives a distinct feature with no known astrophysical background. None of these three ingredients were present in the older analyses.

(c) An advantage of looking for a spectral feature in the diffuse extragalactic gamma-ray background is that regions of the sky can be used where foreground contamination is as low as possible. Previous search strategies, focusing on the Milky Way center or the center of other nearby galaxies, are hampered by the relatively high gamma-ray flux from other sources along these lines of sight.

(d) We note that the GLAST satellite [29] will cover the energy range up to 300 GeV with unprecedented precision. It is possible that most of the measured EGRET flux comes from Active Galactic Nuclei (AGN). Then, the absorption on the infrared background will be severe above 80 GeV for all but the very nearest AGNs. The true diffuse background above 80 GeV may therefore be one or two orders of magnitude smaller than the EGRET extrapolation  $\sim E^{-2.1}$ , with corresponding higher chances of detecting a line signature. Also note that the flux from the  $2\gamma$  line and from continuum gammas in neutralino annihilation are not strongly correlated (except in the case of very pure higgsinos [16]), so it may well be that the line is visible but not the “bump”, and vice versa.

(e) We notice that the spectral features of Fig. 1 would

appear with high significance, for the line it is of the order of  $10\sigma$  for a 5-year exposure with GLAST assuming the background extrapolation  $\sim E^{-2.1}$  given in [26], which becomes  $20\sigma$  if, in analogy with the spectral slope of other cosmic rays, the background above 10 GeV drops like  $E^{-2.7}$  instead. Even if halos have less singular density profiles, such as the cored isothermal sphere, a detectable signature may appear. Alternatively, for the Moore and NFW profiles, models with smaller gamma-ray branching ratios and/or higher masses may be probed.

(f) The relatively broad spectral feature caused by the redshifted gamma-ray line alleviates the demand for very high energy resolution of the detecting instrument put by the previous suggestions of searching for the line in the local Galactic neighbourhood. We find that an energy resolution of 10–20 % is in fact adequate. For GLAST, this means that the effective area can in fact be larger than we have assumed (since a smaller requirement on the energy resolution means that events from a larger part of the field of view of the detector can be used).

(g) It has to be reminded that the strength of the gamma-ray line can be much lower than the examples we chose for Fig. 1, in which case a detection would be correspondingly more difficult. However, in many of those cases the continuum signal may be large. In particular, we find that models compatible with the recent results on the muon  $g-2$  [30] according to the suggested contributions of “new physics” (such as supersymmetry) of [31] all give high values for the continuum gamma-ray flux.

(h) Although the clumpy structure is in the dark matter distribution, and may not have optical counterparts, the rate of the annihilation should scale with the overall matter distribution in the nearby Universe. Thus, once mass maps from, e.g., the Sloan Digital Sky Survey are available, a cross-correlation analysis with the gamma-ray maps should enable a further reduction of Galactic gamma-ray foregrounds.

To conclude, we have suggested a new possible signature for dark matter detection, which employs the clustering properties of Cold Dark Matter as they emerge from  $N$ -body simulations. The upcoming GLAST satellite, and possibly ground based detectors, may have a good chance at detecting the characteristic features, in particular the rise and sudden drop in gamma-ray flux around the WIMP mass produced by annihilation into two photons.

## ACKNOWLEDGEMENTS

L.B. and J.E. wish to thank the Swedish Research Council for financial support. P.U. was supported by the RTN project under grant HPRN-CT-2000-00152. L.B. wants to thank the Institute for Advanced Study, Princeton, for hospitality while this work was completed, and D. Spergel for useful discussions.

- 
- [1] M. Srednicki, S. Theisen and J. Silk, Phys. Rev. Lett. **56**, 263 (1986); Erratum-ibid. **56**, 1883 (1986).
  - [2] S. Rudaz, Phys. Rev. Lett. **56**, 2128 (1986).
  - [3] L. Bergström and H. Snellman, Phys. Rev. D **37**, 3737 (1988).
  - [4] G. Jungman and M. Kamionkowski, Phys. Rev. D **51**, 3121 (1995).
  - [5] L. Bergström and P. Ullio, Nucl. Phys. B **504**, 27 (1997).
  - [6] P. Ullio and L. Bergström, Phys. Rev. D **57**, 1962 (1998).
  - [7] A. Jenkins et al. (The Virgo Consortium), Astrophys. J. **499**, 20 (1998).
  - [8] B. Moore et al., Astrophys. J. **499**, L5 (1998).
  - [9] J.F. Navarro, C.S. Frenk and S.D.M. White, Astrophys. J. **462**, 563 (1996).
  - [10] S. Ghigna et al., Astrophys. J. **544**, 616 (2000).
  - [11] R.A.C. Croft et al., Astrophys. J. **520**, 1 (1999).
  - [12] J.S. Bullock, A.V. Kravtsov and D.H. Weinberg, Astrophys. J. **548**, 33 (2001).
  - [13] B. Moore, astro-ph/0103100 (2001).
  - [14] W.H. Press and P. Schechter, Astrophys. J. **187**, 425 (1974).
  - [15] J. Silk and A. Stebbins, Astrophys. J. **411**, 439 (1993).
  - [16] L. Bergström, J.H. Buckley and P. Ullio, Astropart. Phys. **9**, 137 (1998).
  - [17] L. Bergström, J. Edsjö, P. Gondolo and P. Ullio, Phys. Rev. D **59**, 043506 (1999).
  - [18] E. A. Baltz, C. Briot, P. Salati, R. Taillet and J. Silk, Phys. Rev. D **61**, 023514 (2000).
  - [19] L. Bergström, J. Edsjö and C. Gunnarsson, Phys. Rev. D **63**, 083515 (2001).
  - [20] C. Calcáneo-Roldan and B. Moore, Phys. Rev. D **62**, 123005 (2000).
  - [21] L. Bergström, Rept. Prog. Phys. **63**, 793 (2000).
  - [22] L. Bergström and A. Goobar, *Cosmology and Particle Astrophysics*, Wiley/Praxis (Chichester), 1999.
  - [23] M.H. Salamon and F.W. Stecker, Astrophys. J. **493**, 547 (1998).
  - [24] J.R. Primack, R.S. Somerville, J.S. Bullock and J.E.G. Devriendt, eprint astro-ph/0011475 (2000).
  - [25] DarkSUSY package, homepage <http://www.physto.se/~edsjo/darksusy>. See P. Gondolo, J. Edsjö, L. Bergström, P. Ullio and E. A. Baltz, eprint astro-ph/0012234 (2000).
  - [26] P. Sreekumar et al., Astrophys. J. **494**, 523 (1998).
  - [27] J.S. Bullock et al., Astrophys. J. **550**, 21 (2001).
  - [28] J.E. Gunn, B.W. Lee, I. Lerche, D.N. Schramm and G. Steigman, Astrophys. J. **223**, 1015 (1978); F.W. Stecker, Astrophys. J. **223**, 1032 (1978); J.S. Silk and M. Srednicki, Phys. Rev. Lett. **53**, 624 (1984); Y.-T. Gao, F.W. Stecker and D.B. Cline, Astronomy and Astrophys. **249**, 1 (1991).
  - [29] Gamma-ray Large Area Space Telescope (GLAST), homepage <http://www-glast.stanford.edu>.
  - [30] H.N. Brown et al., Phys. Rev. Lett. **86**, 2227 (2001).
  - [31] W.J. Marciano and A. Czarnecki, eprint hep-ph/0102122 (2001).